Geophysical Research Letters

RESEARCH LETTER
10.1029/2023GL107134

Effect of Long-Range Transported Fire Aerosols on Cloud Condensation Nuclei Concentrations and Cloud Properties at High Latitudes

S. M. Kommula[1], A. Buchholz[1], Y. Gramlich[2,3], T. Mielonen[4], L. Hao[1], I. Pullinen[1], L. Vettikkat[1], A. Ylisirniö[1], J. Joutsensaari[1], S. Schobesberger[1], P. Tiitta[4], A. Leskinen[1,4], D. Hesslin- Rees[2,3], S. L. Haslett[2,3], K. Siegel[2,3], C. Lunder[5], P. Zieger[2,3], R. Krejci[2,3], S. Romakkaniemi[4], C. Mohr[6,7], and A. Virtanen[1]

[1]Department of Technical Physics, University of Eastern Finland, Kuopio, Finland, [2]Department of Environmental Science, Stockholm University, Stockholm, Sweden, [3]Bolin Centre for Climate Research, Stockholm University, Stockholm, Sweden, [4]Finnish Meteorological Institute, Kuopio, Finland, [5]NILU-Norwegian Institute for Air Research, Kjeller, Norway, [6]Laboratory of Atmospheric Chemistry, Paul Scherrer Institute (PSI), Villigen, Switzerland, [7]Department of Environmental System Science, ETH Zurich, Switzerland

Abstract Active vegetation fires in south-eastern (SE) Europe resulted in a notable increase in the number concentration of aerosols and cloud condensation nuclei (CCN) particles at two high latitude locations—the SMEAR IV station in Kuopio, Finland, and the Zeppelin Observatory in Svalbard, high Arctic. During the fire episode aerosol hygroscopicity κ slightly increased at SMEAR IV and at the Zeppelin Observatory κ decreased. Despite increased κ in high CCN conditions at SMEAR IV, the aerosol activation diameter increased due to the decreased supersaturation with an increase in aerosol loading. In addition, at SMEAR IV during the fire episode, in situ measured cloud droplet number concentration (CDNC) increased by a factor of ~7 as compared to non-fire periods which was in good agreement with the satellite observations (MODIS, Terra). Results from this study show the importance of SE European fires for cloud properties and radiative forcing in high latitudes.

Plain Language Summary Wildfires are large sources of aerosol particles and affect human health and climate. Aerosols from fires are transported long distances in the atmosphere and affect the aerosol and cloud properties at places far from the actual sources. In this study, we measured the long-range transported (LRT) fire air masses from south-eastern (SE) Europe at a northern European and a high Arctic site. LRT fire emissions from SE Europe increase the aerosol number and mass loading in Finland and even in the high Arctic. Results show that the effect of fire emissions on aerosol hygroscopicity depends on the properties of both the LRT fires and the background aerosols at a given location. The cloud properties analysis in eastern Finland shows that despite high hygroscopicity and increased CCN activity, the aerosol activation diameter for clouds increased during the fire episode. This is due to the depletion of available water vapor in clouds due to the increased aerosol loading. Satellite observations show an increase in cloud droplet number concentration during the fire episode confirming the effect of LRT fires on cloud properties in eastern Finland. This study can improve the understanding of the effect of LRT fires on aerosol and cloud properties at remote locations.

Key Points:

- Vegetation fires from southern Europe enhance aerosol and cloud condensation nuclei concentrations in northern Europe and the high Arctic
- A contrary trend in aerosol hygroscopicity is observed at these two locations during a strong fire episode as compared to non-fire periods
- Cloud droplet number concentrations in liquid clouds show strong response to fire aerosol both in in situ and satellite observations

Supporting Information:

Supporting Information may be found in the online version of this article.

Correspondence to:

S. M. Kommula and A. Virtanen,
snehitha.kommula@uef.fi;
Annele.virtanen@uef.fi

Citation:

Kommula, S. M., Buchholz, A., Gramlich, Y., Mielonen, T., Hao, L., Pullinen, I., et al. (2024). Effect of long-range transported fire aerosols on cloud condensation nuclei concentrations and cloud properties at high latitudes. *Geophysical Research Letters*, *51*, e2023GL107134. https://doi.org/10.1029/2023GL107134

Received 9 NOV 2023
Accepted 13 MAR 2024

Author Contributions:

Conceptualization: C. Lunder, P. Zieger, A. Virtanen
Formal analysis: S. M. Kommula, A. Buchholz, T. Mielonen, L. Hao, I. Pullinen, L. Vettikkat, A. Ylisirniö, J. Joutsensaari, S. Schobesberger, P. Tiitta, A. Leskinen, D. Hesslin- Rees, S. L. Haslett, K. Siegel, C. Lunder, P. Zieger, R. Krejci, S. Romakkaniemi, C. Mohr, A. Virtanen
Funding acquisition: C. Lunder, P. Zieger, A. Virtanen
Investigation: S. M. Kommula, A. Buchholz, L. Vettikkat, A. Ylisirniö,

1. Introduction

Wildfire emissions are one of the most prominent sources of atmospheric aerosols and have an important impact on air quality, human health, and climate (Andreae, 2019; Bond et al., 2013). Aerosols from fires affect the climate directly by influencing the radiative forcing through scattering and absorption of solar radiation (Crutzen & Andreae, 1990; Haywood & Boucher, 2000) and indirectly by altering cloud properties (Graaf et al., 2022; Sporre et al., 2014; Spracklen et al., 2011). Fire emissions from biomass burning (BB) produce high concentrations of particulate pollutants, such as black carbon (BC) and brown carbon, that absorb incoming solar radiation (Forrister et al., 2015). Particles emitted from BB are typically larger than 100 nm and easy to act as cloud condensation nuclei (CCN) even at low supersaturations (Reid et al., 2005). Remote sensing and in situ measurements have reported that wildfires lead to increased CCN concentration resulting in more reflective clouds with smaller droplet size (Eagan, 1974; Hegg et al., 2012; Jia et al., 2019; Lathem et al., 2013; H. H. Lee & Wang, 2020; Ross et al., 2003).

A. Leskinen, D. Hesslin- Rees, C. Lunder, P. Zieger, R. Krejci, S. Romakkaniemi, C. Mohr, A. Virtanen
Methodology: A. Buchholz, Y. Gramlich, T. Mielonen, L. Hao, I. Pullinen, L. Vettikkat, A. Ylisirniö, J. Joutsensaari, P. Tiitta, A. Leskinen, D. Hesslin- Rees, C. Lunder, P. Zieger, R. Krejci, S. Romakkaniemi, C. Mohr, A. Virtanen
Project administration: C. Lunder, P. Zieger, A. Virtanen
Resources: A. Buchholz, Y. Gramlich, L. Vettikkat, A. Ylisirniö, A. Leskinen, D. Hesslin- Rees, C. Lunder, P. Zieger, R. Krejci, S. Romakkaniemi, C. Mohr, A. Virtanen
Software: A. Buchholz, T. Mielonen, L. Hao, P. Zieger, R. Krejci
Supervision: A. Buchholz, C. Lunder, P. Zieger, R. Krejci, A. Virtanen
Validation: C. Lunder, P. Zieger, A. Virtanen
Writing – original draft: S. M. Kommula
Writing – review & editing: S. M. Kommula, A. Buchholz, Y. Gramlich, T. Mielonen, L. Hao, I. Pullinen, L. Vettikkat, A. Ylisirniö, J. Joutsensaari, S. Schobesberger, P. Tiitta, A. Leskinen, D. Hesslin- Rees, S. L. Haslett, K. Siegel, C. Lunder, P. Zieger, R. Krejci, S. Romakkaniemi, C. Mohr, A. Virtanen

Over the past decade, the frequency of wildfires has increased globally (Jolly et al., 2015; Tyukavina et al., 2022) and the future fire risk is expected to increase further with increasing temperatures (Dupuy et al., 2020; Field et al., 2009; Mccarty et al., 2021; Zheng et al., 2020). Fire emissions can be transported over long distances in the atmosphere and undergo aging which alters their physicochemical properties, such as an increase in the oxidized organic content and hygroscopicity (Hodshire et al., 2019). These chemically transformed aerosols might affect cloud properties differently than fresh BB and wildfire plumes (Laing et al., 2016; Sakamoto et al., 2015; Vakkari, 2014). In addition, long-range transported (LRT) smoke/BC from fires can result in snow melting and increased cloud albedo in the Arctic (Engelmann et al., 2021). Previously, LRT fires from western Russia and southern Europe increased aerosol loadings in Finland and the Arctic (Konovalov et al., 2015; Marelle et al., 2015; Markowicz et al., 2016; Mielonen et al., 2012, 2013; Niemi et al., 2004; Portin et al., 2012; Saarnio et al., 2010; Sillanpää et al., 2005; Stohl et al., 2007).

Few studies reported enhanced cloud droplet number concentration (CDNC) during forest fires for example, in North America, the Amazon rain forest, Pacific northwest (Conrick et al., 2021; Herbert et al., 2021; Makar et al., 2021; Martins & Silva Dias, 2009), and the western U.S. (Twohy et al., 2021). These modeling/aircraft-based/remote sensing studies have focused on fresh BB smoke, which is chemically very different from aged BB air masses. These observations might not represent the response of cloud microphysical properties to LRT fire airmasses. Several other studies characterized the evolution of LRT smoke plumes but are mainly limited to aerosol physical/optical properties and air quality (Ceamanos et al., 2023; Ditas et al., 2018; Moroni et al., 2017; Pöhlker et al., 2018; Shrestha et al., 2022; Zheng et al., 2020).

In this study, we characterized LRT fire air masses in eastern Finland and a high Arctic location during Autumn 2020. We investigate the changes in aerosol properties in both locations, and the effect of LRT fire aerosols on liquid cloud properties in eastern Finland using in situ observations. Additionally, analysis from satellite observations (MODerate Resolution Imaging Spectroradiometer, MODIS (Terra)) was used to investigate cloud response. This is the first study where a strong cloud response to LRT fire aerosol perturbations in liquid clouds are shown using both in situ and satellite observations.

2. Experiments and Methods

Measurements in this study were carried out at the SMEAR IV (Station for Measuring Ecosystem-Atmospheric Relations) in Kuopio, eastern Finland from 15.09.2020 to 24.11.2020 and at the Zeppelin Observatory in Ny-Ålesund, Svalbard from 15.09.2020 to 21.10.2020. The SMEAR IV is located on the top of Puijo tower (62.90°N, 27.65°E; 306 m a.s.l and 225 m above lake level), hereafter referred to as "SMEAR-IV" (Leskinen et al., 2009). Additionally, at ground level (200 m below the SMEAR-IV inlets), a "Puijo ground station" was operated to investigate the differences in aerosol properties when the SMEAR-IV was inside and outside a cloud. The Zeppelin Observatory (78.90°N, 11.88°E) is located on the Zeppelin Mountain at 472 m a.s.l. in Svalbard, hereafter referred to as "Zeppelin" An overview of the observational program at the Zeppelin can be found elsewhere (Platt et al., 2022). The locations of the measurement sites are shown in Figure S1 in Supporting Information S1. Both SMEAR-IV and Zeppelin are inside low-level clouds <10% and ∼15% of the time, respectively, due to their topographic prominence.

At SMEAR-IV (on top of the tower), a twin inlet system was used for aerosol sampling (Figure S2a in Supporting Information S1; Portin et al., 2014). The total inlet sampled aerosol particles and cloud droplets with diameters <40 μm. The interstitial inlet has a PM_1 impactor and measured only non-activated aerosol particles (<1 μm). At the Puijo ground station, an inlet with a $PM_{2.5}$ impactor was used (Figure S2b in Supporting Information S1). More details about this campaign and stations can be found in Calderón et al. (2022). At Zeppelin, a whole air inlet following the ACTRIS recommendation (Platt et al., 2022) was used to sample the aerosol particles and cloud droplets <40 μm (Figure S2c in Supporting Information S1).

The chemical composition of submicron aerosol particles (NR-PM_1; non-refractory particulate matter <1 μm) was measured with a High-Resolution Time-of-Flight Aerosol Mass Spectrometer (HR-ToF-AMS, Aerodyne Research, Inc.) at Puijo ground station and an Aerosol Chemical Speciation Monitor (ACSM, Aerodyne Research, Inc.) at SMEAR-IV and Zeppelin. The aerosol size distribution was measured with Differential Mobility Particle Sizers (DMPS) and equivalent black carbon (eBC) was derived from a Multi-Angle Absorption Photometer (MAAP) at both sites (Texts S1.3–1.4 in Supporting Information S1). Particulate levoglucosan was

measured with a Filter Inlet for Gases and AEROsols coupled to a Chemical Ionisation high-resolution time-of-flight Mass Spectrometer (FIGAERO-CIMS, Aerodyne Research Inc.) using iodide as a reagent ion at Zeppelin.

The aerosol hygroscopicity parameter was derived from the chemical composition data from AMS and ACSM (κ_{chem}) (See Text S1.7, Table S1 in Supporting Information S1), and the obtained κ_{chem} was used to derive the CCN concentration ($N_{CCN\text{-}chem}$) from the measured particle size distribution assuming 0.2% supersaturation applying the κ-Köhler theory (Text S1.8, Table S1 in Supporting Information S1; Petters & Kreidenweis, 2007). Additionally, at SMEAR-IV, N_{CCN} was measured directly with a CCN counter, and the cloud droplet number concentration (CDNC) was calculated from the twin inlet DMPS data (Text S1.4 in Supporting Information S1) (Portin et al., 2014).

Back-trajectory analysis was carried out using the Hybrid Single-Particle Lagrangian Integrated Trajectory model (HYSPLITv5.0.0) (Stein et al., 2015). Information about active fires was retrieved from the Fire Information for Resource Management System (FIRMS) by NASA ("MODIS/Aqua Terra Thermal Anomalies/Fire locations 1 km FIRMS V006 NRT (Vector data)," 2015) (Text S1.5 in Supporting Information S1). Additionally, at SMEAR-IV, satellite observations (MODIS, Terra) were carried out and CDNC was calculated with level-2 cloud products from NASA's Earth data portal (Platnick et al., 2003, 2017) (Text S1.4.5 in Supporting Information S1). More details about the instrumentation and data analysis are presented in Text S1 in Supporting Information S1.

During the campaign, a period with a substantial increase in accumulation mode aerosol number concentration, elevated NR-PM_1 and eBC was observed between 23.09.2020 and 10.10.2020 at SMEAR-IV. The mass concentration of NR-PM_1 and eBC during this period increased by a factor of ∼7 when compared to the campaign average (15.09.2020–24.11.2020), reaching a maxima of 25.4 and 1.6 μg m^{-3}, respectively. Similarly, at Zeppelin, elevated aerosol concentrations were observed between 04.10.2020 and 09.10.2020 with mass concentration of NR-PM_1 and eBC reaching a maximum of 4.5 (5× of campaign average) and 0.41 (∼14× of campaign average) μg m^{-3}, respectively.

Back-trajectory analysis shows that for these periods of elevated concentrations, more than 60% of the time the air masses came from south-eastern (SE) Europe where active fires from vegetation/grasslands were detected based on FIRMS (Figure S3 in Supporting Information S1). Combining this with the observation of biomass burning tracer compound (discussed in Section 3.1), these episodes are referred to as the "Fire episode" (Text S2.1 in Supporting Information S1). Based on back-trajectory analysis, we associate the detected plumes at both sites with the same fire region (Figures S4a and S4c in Supporting Information S1). The fire emissions were estimated to be ∼1–4 days old when they arrived SMEAR-IV (Figure S5 in Supporting Information S1) and ∼4–8 days at Zeppelin, that is, they were more aged at Zeppelin than at SMEAR-IV.

To quantify the effect of the LRT fire emissions on the aerosol and cloud properties, we defined a reference period for both sites representing unperturbed conditions. For SMEAR-IV, air masses coming from the Atlantic and Arctic (A/A) regions over Scandinavia were relatively clean and considered as typical air masses at this location (Figure S4b in Supporting Information S1). The corresponding periods are classified as non-fire period ("NF period") (Text S2.1 in Supporting Information S1). For Zeppelin, the back-trajectory analysis revealed two other air mass source regions: (a) marine air masses from the North Atlantic (NA, Figure S4d in Supporting Information S1) and (b) air masses coming from the Arctic and Greenland (AG, Figure S4e in Supporting Information S1). The aerosol concentrations were below the ACSM detection limit during NA periods and could not be used. Thus, we used AG periods as the non-fire period (NF).

3. Results and Discussion

3.1. Effect of Long Range Transported Fire Emission on Aerosol Composition

An overview of the aerosol properties at SMEAR-IV and Zeppelin is shown in Figure 1. At SMEAR-IV, the average mass concentrations of NR-PM_1 and eBC during the campaign were 3.5 ± 4.1 μg m^{-3} and 0.2 ± 0.3 μg m^{-3}, respectively. At Zeppelin, the average (±standard deviation) NR-PM_1 and eBC mass concentrations observed for the whole campaign were 0.9 ± 1.1 μg m^{-3} and 0.03 ± 0.07 μg m^{-3}, respectively. During the campaign, at SMEAR-IV, the weekly average temperature (±standard deviation) was 11 ± 2°C during the start of the campaign, decreasing gradually to 2 ± 3°C during the final week. At Zeppelin, the ambient temperature was ranging from +7°C to −10°C during the campaign (Text S1.3.3 in Supporting Information S1).

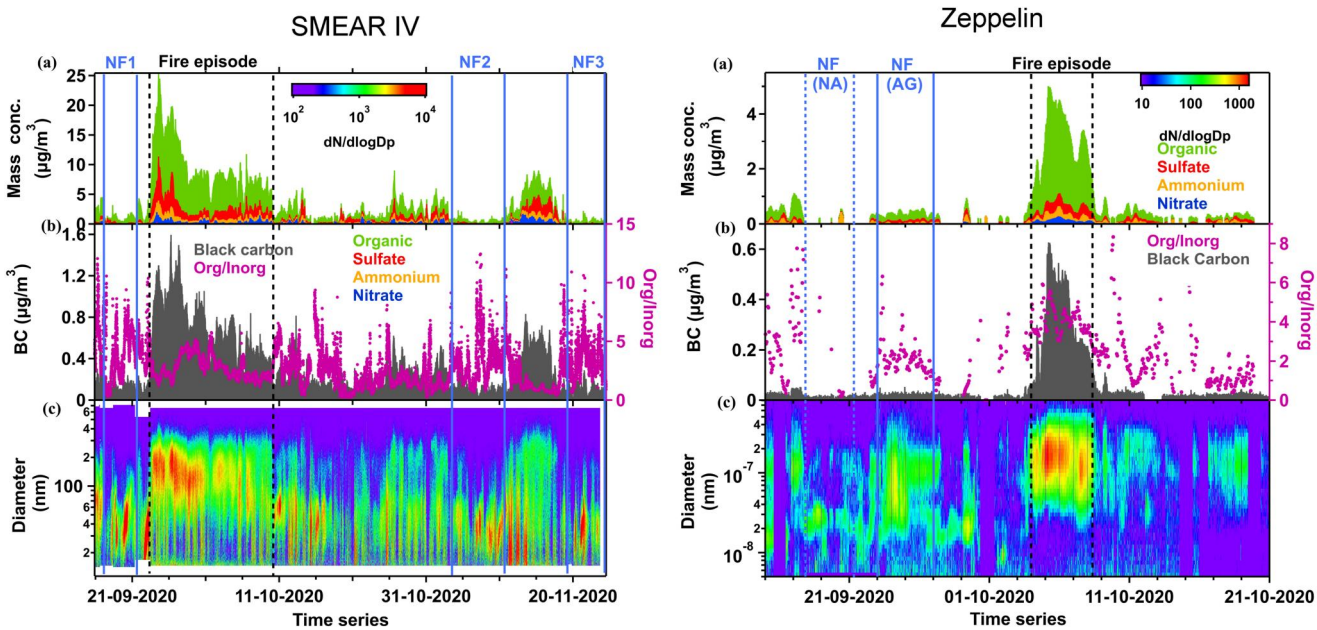

Figure 1. Overview of (a) mass concentration of Non-Refractory Particulate Matter <1 μm (b) equivalent Black carbon, organic/inorganic mass ratio and (c) size distribution, at SMEAR-IV (left) and Zeppelin (right) for the measurement period. The fire episode is marked with black dashed lines and blue lines indicate the non-fire periods. Note the difference in the scale of the *y*-axis and color bar for both sites.

The campaign average NR-PM_1 chemical composition of measured aerosol particles at SMEAR-IV is dominated by organics (67%) followed by sulfate (20%), ammonium (7%), and nitrate (6%). During the NF period, the contribution of inorganics and organics was 21% and 79% (Figure 2a). For the fire episode, the fraction of inorganics increased to 29%, while organics contributed ~71% of the total NR-PM_1 mass. This increase of the

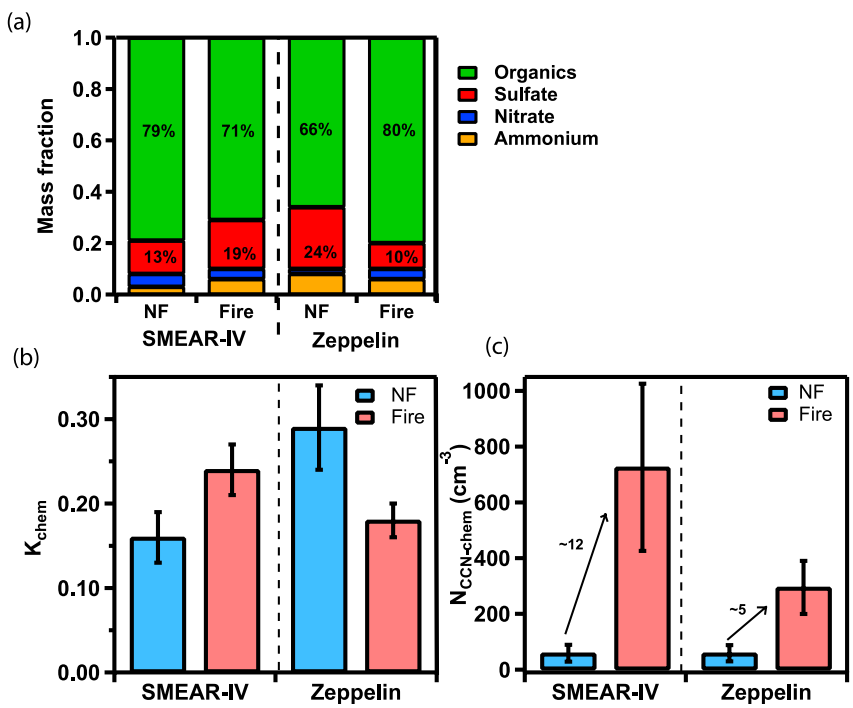

Figure 2. (a) The mass fraction of aerosol composition for the fire episode and NF periods; (b) average κ_{chem} ($\kappa_{org} = 0.07$) and (c) average $N_{CCN\text{-}chem}$ for the cloud events during fire and NF periods at SMEAR-IV and Zeppelin.

inorganic fraction could be partly attributed to fire emissions and partly to the influence of anthropogenic emissions. The fire air masses were transported to SMEAR-IV through central and eastern Europe, and heavily affected by industrial, and other terrestrial emissions. Therefore, air masses arriving at SMEAR-IV during the fire episode are affected by both fires from SE Europe and other emissions along the airmass transport route. Interestingly, at Zeppelin, we observed the opposite trend for the inorganic and organic contribution: during the NF period, aerosols had a higher inorganic fraction (44%) than during the fire episode (20%) (Figure 2a). High inorganic mass fractions at Zeppelin during the clean period (NF) are likely due to the influence of marine emissions (Adachi et al., 2022). During the fire episode, the organic mass fraction increased substantially (from 66% to 80%), indicating the impact of the fire emissions and other terrestrial sources. The observed difference in the contribution of organic and inorganic compounds during fire episodes emphasize the importance of background aerosol composition at these locations, as the observed aerosol properties are the result of the superposition of two (background and fire related) aerosol populations.

For the fire episode, an increase in the particle-phase concentration of levoglucosan, a tracer compound for BB, was observed at Zeppelin directly by FIGAERO-CIMS ($C_6H_{10}O_5I^-$) and at SMEAR-IV as $C_2H_4O_2^+$ (m/z 60) with the AMS (Figure S6 in Supporting Information S1). This further confirms the influence of BB emissions during this episode. However, the mass fraction of levoglucosan f_{60} (m/z 60/total organic signal) did not increase. This is due to the long aging time of the fire emissions: while the initial levoglucosan is consumed by atmospheric aging (average lifetime 0.7—2.2 days, (Li et al., 2021)), new organic material from various sources along the transport route is added to the fire aerosols. Both effects decrease the contribution of the tracer suggesting that the mass ratio of the AMS/ACSM tracer to total organics is not a suitable indicator for aged fire aerosols (Cubison et al., 2011; Hennigan et al., 2010).

For further analysis of composition changes related to the LRT fire aerosols, a positive matrix factorization (PMF) analysis was performed for the high-resolution (HR) organic mass spectra data from AMS at Puijo ground station. The details of the chosen 5-factor solution are described in Text S2.2 in Supporting Information S1 (Figures S7–S9 in Supporting Information S1). The factors were classified as two local (HOA—hydrocarbon-like Organic Aerosol and LO-OOA—less oxidized-oxygenated OA) and three LRT (MO-OOA—more oxidized-oxygenated OA) factors. The majority of the $C_2H_4O_2^+$ ion (m/z 60) signal was attributed to the LRT factors. Additionally, the ratio of m/z 60 to m/z 73 (another BB marker) is ∼1.2 for these factors which is in the range identified for wood burning OA and BBOA (Xu et al., 2020).

The mass contribution of the five PMF-factors for different periods is shown in Figure S9 in Supporting Information S1. During NF periods, the organics are dominated by the local factors with contributions of HOA of 11% and LO-OOA of 42% followed by MO-OOA (LRT factors) (47%). During the fire episode, the contributions from local sources decreased to 6% HOA and 5% LO-OOA while the contribution of MO-OOA increased to 89% indicating the substantial effect of LRT fire emissions in altering the organic composition. OOA are typically more hygroscopic and have higher CCN activity (Duplissy et al., 2011; Rejano et al., 2023) than freshly emitted OA compounds. The effect of increased OOA fraction during the fire episode on aerosol hygroscopicity and CCN properties at SMEAR-IV is discussed in Section 3.3.

Unfortunately, the detailed organic composition at Zeppelin is not yet available for such a comparison.

3.2. Influence of LRT Fire Emissions on Aerosol Hygroscopicity, CCN Activity, and Cloud Properties

3.2.1. Aerosol Hygroscopicity and CCN Activity

To understand the effect of LRT fire aerosols on cloud properties, we first studied the average aerosol properties during cloud events for the fire and NF periods. No clouds were detected during the NF period at Zeppelin. Thus, we used the whole NF period average values as a proxy.

Aerosol hygroscopicity is represented by the hygroscopicity parameter κ. Most inorganic aerosol species (e.g., salts) are more hygroscopic with larger κ values ($\kappa = 0.4 - 1.3$) than organic compounds (typically, $\kappa = 0.05 - 0.2$) (Petters & Kreidenweis, 2007; Suda et al., 2012). κ values of organic compounds (κ_{org}) usually increase with oxidation level of OA (Jimenez et al., 2009; Kuang et al., 2020; Wu et al., 2016) and can be expressed as a function of O:C ratio ($\kappa_{org} = f(\text{O:C})$) (Chang et al., 2010; Rickards et al., 2013). For Zeppelin, the elemental composition data is not available yet. Thus, we used a constant value for κ_{org}. For the Puijo data, we calculated κ_{chem} (κ calculated from chemical composition data) with both $\kappa_{org} = f(\text{O:C})$ and $\kappa_{org} = 0.07$. Using $\kappa_{org} = f(\text{O:C})$

Table 1
Average Values and Standard Deviation of Fraction of Organics (f_{org}), κ_{chem}, $N_{CCN\text{-}chem}$ and N_{tot}, Cloud Activation Diameter (D_{act}) and CDNC for Fire and NF Periods at SMEAR-IV and Zeppelin

	SMEAR-IV		Zeppelin	
	Fire episode	NF period	Fire episode	NF period
f_{org}	0.71 ± 0.16	0.79 ± 0.27	0.80 ± 0.05	0.66 ± 0.08
κ_{chem} (κ_{org} = 0.07)	0.24 ± 0.03	0.16 ± 0.03	0.18 ± 0.02	0.29 ± 0.05
κ_{chem} (κ_{org} = f(O:C))	0.28 ± 0.03	0.19 ± 0.03	–	–
$N_{CCN\text{-}chem}$ (cm^{-3})	726 ± 300	59 ± 30	331 ± 95	59 ± 29
N_{tot} (cm^{-3})	6,070 ± 3,537	4,500 ± 3,623	491 ± 133	169 ± 94
D_{act} (nm) (Twin inlet)	139 ± 21	107 ± 30	–	–
CDNC (cm^{-3}) (Twin inlet)	521 ± 198	77 ± 24	–	–
CDNC (cm^{-3}) (Satellite)	555 ± 139 (24 Sep)	88 ± 32 (31 Oct)	–	–

Note. Satellite observations of CDNC are for the case studies on 24.09.2020 and 31.10.2020.

results in overall higher κ_{chem} values (Table 1), but the difference between the fire and NF period values is similar for both methods. Thus, we used the κ_{chem} calculated with constant κ_{org} in the following section to enable the direct comparison between the two stations.

κ_{chem} at SMEARV-IV was slightly higher during the fire episode when compared to NF period (increased to 0.24 from 0.16) (Figure 2b). This is due to the higher fraction of inorganic compounds (Figure 2a) and MO-OOA (Table 1; Figure S9 in Supporting Information S1), during the fire episode when compared to the NF period. In contrast, at Zeppelin, κ_{chem} decreased to 0.18 during the fire episode from 0.29 in NF period. Aerosols at this location are expected to be mostly marine influenced and unaffected by anthropogenic emissions at this season (Autumn). Thus, the aerosols are rich in inorganics and more hygroscopic, and the addition of any OA could only reduce the hygroscopicity. This observation further highlights the role of the background conditions, that is, whether LRT fire aerosols increase or decrease the aerosol hygroscopicity at a specific location. Note that the reported κ_{chem} values are most likely underestimated for Zeppelin as the ACSM cannot quantify a very hygroscopic compound, sodium chloride (κ = 1.28; Petters & Kreidenweis, 2007) from sea salt, which may be a major constituent in this environment. A mass closure study was performed to obtain a rough estimate of the NaCl concentration (Text S2.2 in Supporting Information S1). κ_{chem} values including NaCl were much higher during the NF period than the Fire episode (Figure S10 and Table S2 in Supporting Information S1), further confirming that the fire air masses reduced the aerosol hygroscopicity at Zeppelin.

The fraction of aerosols that can act as CCN at a given supersaturation depends on the aerosol number size distribution and hygroscopicity. Some studies reported the significance of hygroscopicity (Takeishi et al., 2020; Väisänen et al., 2016) while others found the number/size effect to be dominant (Dusek et al., 2006; Schmale et al., 2018). Jung et al. (2018) reported an increase in N_{CCN} at Zeppelin with an increase in aerosol number concentration (N_{tot}). During the fire episode the accumulation mode particle concentration increased at both sites. At SMEAR-IV, N_{tot} increased by a factor of ∼1.3 during the fire episode, while at Zeppelin N_{tot} increased by ∼3-fold (Table 1). Consequently, the N_{CCN} (0.2% SS) also increased substantially during the fire episode at both sites. But the magnitude of the increase in N_{CCN} at SMEAR-IV is much larger (∼12-fold) than that observed at Zeppelin (∼5.6 -fold) (Figure 2c). This is partly explained by the opposite response in the particle hygroscopicity between fire and NF periods at these locations, indicating the importance of particle hygroscopicity in CCN activation. To quantify the contribution of chemical composition (hygroscopicity) on CCN change, we calculated N_{CCN} using κ_{chem} values from the NF period and the size distributions measured during the fire episode (Text S2.3 in Supporting Information S1). Results show that at SMEAR-IV, the increase in κ_{chem} increased N_{CCN} by 25%, whereas at Zeppelin the reduction in κ_{chem} decreased N_{CCN} by 13% [see Tables S3 and S4 in Supporting Information S1]. This shows that the chemical composition change due to LRT fire aerosol has a considerable effect on N_{CCN} at both sites.

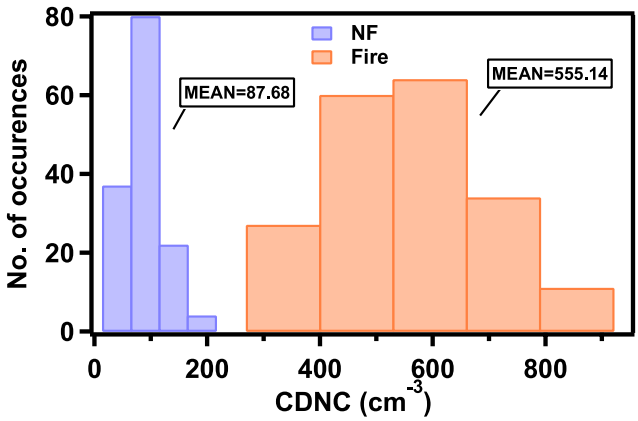

Figure 3. Histograms of CDNC calculated from satellite observations at SMEAR-IV representing a NF (31.10.2020, blue) and a fire period case (24.09.2020, orange). The mean values are indicated.

3.2.2. Cloud Microphysical Properties

The formation of cloud droplets depends on updraft velocity at a location, temperature, particle size, number concentration, and chemical composition. These parameters influence the smallest diameter of the particles that are activated into cloud droplets, referred to as activation diameter (D_{act}). At SMEAR-IV, D_{act} can be measured directly with the twin inlet system when the station is in low level clouds (i.e., for a cloud event, Text S1.2 in Supporting Information S1). For a given supersaturation, increasing hygroscopicity lowers the dry particle diameter required for the activation. However, in this study despite higher κ_{chem} values during the fire episode, the average D_{act} (139 ± 21 nm) is higher than that in the NF period (107 ± 30 nm) (Table 1). This is due to the depletion of available water vapor as the higher number of particles in the accumulation mode consumes more of the available water vapor through water uptake during the activation process, lowering the apparent supersaturation. Additionally, comparing NF periods and the fire episode, we observed a ∼7-fold increase of average CDNC (77 ± 24 cm^{-3} to 521 ± 198 cm^{-3}) while $N_{CCN\text{-}chem}$ increased by an order of magnitude (∼12×). This discrepancy between the predicted ($N_{CCN\text{-}chem}$) and measured values (CDNC) is a further indication of the decreased apparent supersaturation due to high CCN concentration during cloud formation. This process was investigated in more detail using large eddy simulations in Calderón et al. (2022).

To further investigate the feedback of increased CCN concentration on supersaturation, we examined the relationship of the measured cloud droplet concentration (CDNC) and N_{100} (number concentration of particles >100 nm) at the SMEAR-IV (Figure S11a in Supporting Information S1) and compared it to an existing data set measured over the North Atlantic (Ramanathan et al., 2001). There is a linear increase in CDNC with N_{100} for particle concentrations up to ∼750 cm^{-3}. For higher N_{100} values driven by fire airmass influence, the curve flattens due to the depletion of water vapor. Figure S11b in Supporting Information S1 illustrates the effect of inorganic compounds like sulfate on observed CDNC for this campaign and the existing data sets (McCoy et al., 2018), showing that CDNC observed during the fire episode are notably higher than the previous data. The reason for this can be the differences in meteorological conditions or methodology: in situ measurements at SMEAR-IV define CDNC at the cloud base where activation takes place, while satellite captures CDNC at the cloud top (Klingebiel et al., 2015).

Unfortunately, there are no D_{act} and CDNC data at Zeppelin for the investigated time period due to instrument issues. However, recent study by Freitas et al. (2023) observed high contribution of warm ice nuclei particles (INP) for the same fire episode. Thus, not only liquid clouds but also INP properties can be influenced by LRT aerosol from biomass burning. A long term study of cloud residual number concentrations in Arctic low-level clouds, reported D_{act} for liquid clouds (T > 0°C) in the range of 50–78 nm and inferred a relationship of decreasing D_{act} with decreasing N_{tot} (Karlsson et al., 2021), similar to observations at SMEAR-IV.

3.3. Satellite Observations in SMEAR-IV

The effect of the LRT fire aerosols on liquid-cloud properties was further investigated using satellite (MODIS (Terra)) observations at SMEAR-IV. Two case studies were selected during cloud events representing NF (31.10.2020) and fire periods (24.09.2020). During these days, there were no cloud layers above the low-level clouds providing perfect conditions for the analysis of low-level cloud microphysical properties. The histograms for median CDNC retrieved from MODIS for the two case days are shown in Figure 3. The average CDNC increased by a factor of ∼6.8 (from 87 to 555 cm^{-3}) for the fire cloud case when compared to that of the NF cloud case. Overall, our results show that the cloud response to elevated aerosol concentrations during fire episode observed with MODIS seems to be consistent with the in situ observations (Table 1) with very good agreement of the derived parameters.

4. Summary and Conclusions

In this study, we characterized the impact of long-range transported (LRT) fire aerosols from south-eastern Europe on aerosol and cloud properties at two locations. One is in a semi-urban environment in northern

Europe (SMEAR-IV) and the other one is in the high Arctic (Zeppelin) where the background aerosol concentrations are relatively low. The fire episode and representative non-fire (NF) periods were analyzed and the results from both locations were compared. LRT fire aerosols substantially increased the aerosol and CCN concentrations at both locations. Our results suggest that the effect of LRT fire aerosols on aerosol composition and hygroscopicity is driven by the properties of both the LRT fire plumes and the background aerosols. That is, in the high Arctic where marine aerosols are dominating in Autumn and the inorganic fraction of aerosol is relatively high, the hygroscopicity decreases with LRT fire airmass influence, while in the semi-urban northern European location, the opposite is seen due to an increase in the inorganic and oxidized OA fraction during the fire episode. Consequently, the magnitude of increase in CCN concentration during the fire episode is larger at SMEAR-IV than at Zeppelin, suggesting the importance of the hygroscopicity effect for CCN activation under these circumstances. Further, elevated CCN concentration at SMEAR-IV resulted in an increase in cloud activation diameter despite the concurrent increase in hygroscopicity due to the depletion of water vapor during the fire episode.

In situ measurements and satellite observations from MODIS (Terra) at SMEAR-IV showed enhanced CDNC during the fire episode. We found a good agreement between satellite analysis and in situ measurements, when there are no cloud layers above the investigated low-level liquid clouds. The elevated CDNC during LRT fire-influenced air masses may alter the radiative forcing and cloud albedo (Twomey effect) as well as affect cloud coverage and lifetime. Therefore, we highlight the impact of LRT fire aerosols on CCN and cloud properties particularly at remote locations, where cloud activation can be aerosol-limited. We also point to the need to study (aged) fire emissions in more detail, especially considering the projected increasingly dry conditions in the upcoming decades.

Data Availability Statement

The measurement data of aerosol size and chemical composition for SMEAR-IV and Zeppelin used in this manuscript is available at Kommula et al. (2023). Satellite observations for CDNC calculations: The Terra/MODIS Aerosol Cloud Water Vapor Ozone Daily L3 Global 1 Deg. CMG data set was acquired from the Level-1 and Atmosphere Archive and Distribution System (LAADS) Distributed Active Archive Center (DAAC), located in the Goddard Space Flight Center in Greenbelt, Maryland (Platnick et al., 2017). Data for active fires is available at the fire information for resource management system (FIRMS) by NASA (MODIS/Aqua Terra Thermal Anomalies/Fire locations 1km FIRMS V006 NRT (Vector data), 2015).

Acknowledgments

We thank all technical and scientific staff at University of Eastern Finland (UEF), Stockholm University, Norwegian Institute for Air Research (NILU) and Norwegian Polar Institute (NPI), involved in conducting the measurement campaigns at SMEAR IV and Zeppelin Observatory. We also thank Gang Chen (Imperial, UK) for his help with the Zeppelin ACSM data. This work was supported by the European Union's Horizon 2020 research and innovation program under Grant 821205 (FORCeS), and the Knut and Alice Wallenberg (KAW) foundation (WAF project CLOUDFORM, Grant 2017.0165). This work was also supported by the University of Eastern Finland (Doctoral Program in Environmental Physics, Health, and Biology), the Academy of Finland Flagship programme (Grant 337550), and the Research Council of Finland project SHARPCLOUD (Grant 347968) and the Research Council of Finland (project number 339885).

References

Adachi, K., Tobo, Y., Koike, M., Freitas, G., Zieger, P., & Krejci, R. (2022). Composition and mixing state of Arctic aerosol and cloud residual particles from long-term single-particle observations at Zeppelin Observatory, Svalbard. *Atmospheric Chemistry and Physics*, *22*(21), 14421–14439. https://doi.org/10.5194/acp-22-14421-2022

Andreae, M., & Merlet, P. (2019). Emission of trace gases and aerosols from biomass burning. Global Biogeochemical. *Atomospheric Chemistry and Physics*, *15*(4), 955–966. https://doi.org/10.1029/2000gb001382

Bond, T. C., Doherty, S. J., Fahey, D. W., Forster, P. M., Berntsen, T., Deangelo, B. J., et al. (2013). Bounding the role of black carbon in the climate system: A scientific assessment. *Journal of Geophysical Research: Atmospheres*, *118*(11), 5380–5552. https://doi.org/10.1002/jgrd.50171

Calderón, S. M., Tonttila, J., Buchholz, A., Joutsensaari, J., Komppula, M., Leskinen, A., et al. (2022). Aerosol-stratocumulus interactions: Towards a better process understanding using closures between observations and large eddy simulations. *Atmospheric Chemistry and Physics*, *22*(18), 12417–12441. https://doi.org/10.5194/acp-22-12417-2022

Ceamanos, X., Coopman, Q., George, M., Riedi, J., Parrington, M., & Clerbaux, C. (2023). Remote sensing and model analysis of biomass burning smoke transported across the Atlantic during the 2020 Western US wildfire season. *Scientific Reports*, *13*(1), 1–12. https://doi.org/10.1038/s41598-023-39312-1

Chang, R. Y. W., Slowik, J. G., Shantz, N. C., Vlasenko, A., Liggio, J., Sjostedt, S. J., et al. (2010). The hygroscopicity parameter (κ) of ambient organic aerosol at a field site subject to biogenic and anthropogenic influences: Relationship to degree of aerosol oxidation. *Atmospheric Chemistry and Physics*, *10*(11), 5047–5064. https://doi.org/10.5194/acp-10-5047-2010

Conrick, R., Mass, C. F., Boomgard-Zagrodnik, J. P., & Ovens, D. (2021). The influence of wildfire smoke on cloud microphysics during the September 2020 Pacific northwest wildfires. *Weather and Forecasting*, 1519–1536. https://doi.org/10.1175/waf-d-21-0044.1

Crutzen, P. J., & Andreae, M. O. (1990). Biomass burning in the tropics: Impact on atmospheric chemistry and biogeochemical cycles. In *Renewable energy: Four volume set, 4–4* (pp. 246–267). https://doi.org/10.4324/9781315793245-133

Cubison, M. J., Ortega, A. M., Hayes, P. L., Farmer, D. K., Day, D., Lechner, M. J., et al. (2011). Effects of aging on organic aerosol from open biomass burning smoke in aircraft and laboratory studies. *Atmospheric Chemistry and Physics*, *11*(23), 12049–12064. https://doi.org/10.5194/acp-11-12049-2011

Ditas, J., Ma, N., Zhang, Y., Assmann, D., Neumaier, M., Riede, H., et al. (2018). Strong impact of wildfires on the abundance and aging of black carbon in the lowermost stratosphere. *Proceedings of the National Academy of Sciences of the United States of America*, *115*(50), E11595–E11603. https://doi.org/10.1073/pnas.1806868115

Duplissy, J., De Carlo, P. F., Dommen, J., Alfarra, M. R., Metzger, A., Barmpadimos, I., et al. (2011). Relating hygroscopicity and composition of organic aerosol particulate matter. *Atmospheric Chemistry and Physics*, *11*(3), 1155–1165. https://doi.org/10.5194/acp-11-1155-2011

Dupuy, J. L., Fargeon, H., Martin-StPaul, N., Pimont, F., Ruffault, J., Guijarro, M., et al. (2020). Climate change impact on future wildfire danger and activity in southern Europe: A review. *Annals of Forest Science*, *77*(2), 35. https://doi.org/10.1007/s13595-020-00933-5

Dusek, U., Frank, G. P., Hildebrandt, L., Curtius, J., Schneider, J., Walter, S., et al. (2006). Size matters more than chemistry for cloud-nucleating ability of aerosol particles. *Science*, *312*(5778), 1375–1378. https://doi.org/10.1126/science.1125261

Eagan, R., Hobbs, P. V., & Radke, L. F. (1974). Measurements of cloud condensation nuclei and cloud droplet size distributions in the vicinity of forest fires. *Journal of Applied Meteorology*, *13*(5), 553–557. https://doi.org/10.1175/1520-0450(1974)013%3C0553:MOCCNA%3E2.0.CO;2

Engelmann, R., Ansmann, A., Ohneiser, K., Griesche, H., Radenz, M., Hofer, J., et al. (2021). Wildfire smoke, Arctic haze, and aerosol effects on mixed-phase and cirrus clouds over the North Pole region during MOSAiC: An introduction. *Atmospheric Chemistry and Physics*, *21*(17), 13397–13423. https://doi.org/10.5194/acp-21-13397-2021

Field, R. D., Van Der Werf, G. R., & Shen, S. S. P. (2009). Human amplification of drought-induced biomass burning in Indonesia since 1960. *Nature Geoscience*, *2*(3), 185–188. https://doi.org/10.1038/ngeo443

Forrister, H., Liu, J., Scheuer, E., Dibb, J., Ziemba, L., Thornhill, K. L., et al. (2015). Evolution of brown carbon in wildfire plumes. *Geophysical Research Letters*, *42*(11), 4623–4630. https://doi.org/10.1002/2015GL063897

Freitas, G. P., Adachi, K., Conen, F., Heslin-rees, D., Tobo, Y., Yttri, K. E., & Zieger, P. (2023). Regionally sourced bioaerosols drive high-temperature ice nucleating particles in the Arctic. *Nature*, 23–26. https://doi.org/10.1038/s41467-023-41696-7

Graaf, M. D., Sarna, K., Brown, J., Tenner, E., Schenkels, M., & Donovan, P. (2022). Aerosol first indirect effect of African smoke in marine stratocumulus clouds over Ascension Island, South Atlantic Ocean. *Atmospheric Chemistry & Physics Discussions*, *2*, 1–24.

Haywood, J., & Boucher, O. (2000). Estimates of the direct and indirect radiative forcing due to tropospheric aerosols: A review. *Reviews of Geophysics*, *38*(4), 513–543. https://doi.org/10.1029/1999RG000078

Hegg, D. A., Covert, D. S., Jonsson, H. H., & Woods, R. K. (2012). A simple relationship between cloud drop number concentration and precursor aerosol concentration for the regions of Earth's large marine stratocumulus decks. *Atmospheric Chemistry and Physics*, *12*(3), 1229–1238. https://doi.org/10.5194/acp-12-1229-2012

Hennigan, C. J., Sullivan, A. P., Collett, J. L., & Robinson, A. L. (2010). Levoglucosan stability in biomass burning particles exposed to hydroxyl radicals. *Geophysical Research Letters*, *37*(9), 2–5. https://doi.org/10.1029/2010GL043088

Herbert, R., Stier, P., & Dagan, G. (2021). Isolating large-scale smoke impacts on cloud and precipitation processes over the Amazon with convection permitting resolution. *Journal of Geophysical Research: Atmospheres*, *126*(13). https://doi.org/10.1029/2021JD034615

Hodshire, A. L., Akherati, A., Alvarado, M. J., Brown-Steiner, B., Jathar, S. H., Jimenez, J. L., et al. (2019). Aging effects on biomass burning aerosol mass and composition: A critical review of field and laboratory studies. *Environmental Science and Technology*, *53*(17), 10007–10022. https://doi.org/10.1021/acs.est.9b02588

Jia, H., Ma, X., Yu, F., Liu, Y., & Yin, Y. (2019). Distinct impacts of increased aerosols on cloud droplet number concentration of stratus/stratocumulus and cumulus. *Geophysical Research Letters*, *46*(22), 13517–13525. https://doi.org/10.1029/2019GL085081

Jimenez, J. L., Canagaratna, M. R., Donahue, N. M., Prevot, A. S. H., Zhang, Q., Kroll, J. H., et al. (2009). Evolution of organic aerosols in the atmosphere. *Science*, *326*(5959), 1525–1529. https://doi.org/10.1126/science.1180353

Jolly, W. M., Cochrane, M. A., Freeborn, P. H., Holden, Z. A., Brown, T. J., Williamson, G. J., & Bowman, D. M. J. S. (2015). Climate-induced variations in global wildfire danger from 1979 to 2013. *Nature Communications*, *6*, 1–11. https://doi.org/10.1038/ncomms8537

Jung, C. H., Yoon, Y. J., Kang, H. J., Gim, Y., Lee, B. Y., Ström, J., et al. (2018). The seasonal characteristics of cloud condensation nuclei (CCN) in the arctic lower troposphere. *Tellus Series B Chemical and Physical Meteorology*, *70*(1), 1–13. https://doi.org/10.1080/16000889.2018.1513291

Karlsson, L., Krejci, R., Koike, M., Ebell, K., & Zieger, P. (2021). A long-term study of cloud residuals from low-level Arctic clouds. *Atmospheric Chemistry and Physics*, *21*(11), 8933–8959. https://doi.org/10.5194/acp-21-8933-2021

Klingebiel, M., De Lozar, A., Molleker, S., Weigel, R., Roth, A., Schmidt, L., et al. (2015). Arctic low-level boundary layer clouds: In situ measurements and simulations of mono- and bimodal supercooled droplet size distributions at the top layer of liquid phase clouds. *Atmospheric Chemistry and Physics*, *15*(2), 617–631. https://doi.org/10.5194/acp-15-617-2015

Kommula, S. M., Buchholz, A., Gramlich, Y., Mielonen, T., Mohr, C., & Virtanen, A. (2023). Effect of long-range transported fire aerosols on cloud condensation nuclei concentrations and cloud properties at high latitudes [Dataset]. *Zenodo*. https://doi.org/10.5281/zenodo.10786938

Konovalov, I. B., Beekmann, M., Berezin, E. V., Petetin, H., Mielonen, T., Kuznetsova, I. N., & Andreae, M. O. (2015). The role of semi-volatile organic compounds in the mesoscale evolution of biomass burning aerosol: A modeling case study of the 2010 mega-fire event in Russia. *Atmospheric Chemistry and Physics*, *15*(23), 13269–13297. https://doi.org/10.5194/acp-15-13269-2015

Kuang, Y., He, Y., Xu, W., Zhao, P., Cheng, Y., Zhao, G., et al. (2020). Distinct diurnal variation in organic aerosol hygroscopicity and its relationship with oxygenated organic aerosol. *Atmospheric Chemistry and Physics*, *20*(2), 865–880. https://doi.org/10.5194/acp-20-865-2020

Laing, J. R., Jaffe, D. A., & Hee, J. R. (2016). Physical and optical properties of aged biomass burning aerosol from wildfires in Siberia and the Western USA at the Mt. Bachelor Observatory. *Atmospheric Chemistry and Physics*, *16*(23), 15185–15197. https://doi.org/10.5194/acp-16-15185-2016

Lathem, T. L., Beyersdorf, A. J., Thornhill, K. L., Winstead, E. L., Cubison, M. J., Hecobian, A., et al. (2013). Analysis of CCN activity of Arctic aerosol and Canadian biomass burning during summer 2008. *Atmospheric Chemistry and Physics*, *13*(5), 2735–2756. https://doi.org/10.5194/acp-13-2735-2013

Lee, H. H., & Wang, C. (2020). The impacts of biomass burning activities on convective systems over the Maritime Continent. *Atmospheric Chemistry and Physics*, *20*(4), 2533–2548. https://doi.org/10.5194/acp-20-2533-2020

Leskinen, A., Portin, H., Komppula, M., Miettinen, P., Arola, A., Lihavainen, H., et al. (2009). Overview of the research activities and results at Puijo semi-urban measurement station. *Boreal Environment Research*, *14*(4), 576–590.

Li, Y., Fu, T. M., Yu, J. Z., Feng, X., Zhang, L., Chen, J., et al. (2021). Impacts of chemical degradation on the global budget of atmospheric levoglucosan and its use as a biomass burning tracer. *Environmental Science and Technology*, *55*(8), 5525–5536. https://doi.org/10.1021/acs.est.0c07313

Makar, P. A., Akingunola, A., Chen, J., Pabla, B., Gong, W., Stroud, C., et al. (2021). Forest-fire aerosol-weather feedbacks over western North America using a high-resolution, online coupled air-quality model. *Atmospheric Chemistry and Physics*, *21*(13), 10557–10587. https://doi.org/10.5194/acp-21-10557-2021

Marelle, L., Raut, J. C., Thomas, J. L., Law, K. S., Quennehen, B., Ancellet, G., et al. (2015). Transport of anthropogenic and biomass burning aerosols from Europe to the Arctic during spring 2008. *Atmospheric Chemistry and Physics*, *15*(7), 3831–3850. https://doi.org/10.5194/acp-15-3831-2015

Markowicz, K. M., Pakszys, P., Ritter, C., Zielinski, T., Udisti, R., Cappelletti, D., et al. (2016). Impact of North American intense fires on aerosol optical properties measured over the European Arctic in July 2015. *Journal of Geophysical Research: Atmospheres*, *121*(24), 14487–14512. https://doi.org/10.1002/2016JD025310

Martins, J. A., & Silva Dias, M. A. F. (2009). The impact of smoke from forest fires on the spectral dispersion of cloud droplet size distributions in the Amazonian region. *Environmental Research Letters*, *4*(1), 015002. https://doi.org/10.1088/1748-9326/4/1/015002

Mccarty, J. L., Aalto, J., Paunu, V. V., Arnold, S. R., Eckhardt, S., Klimont, Z., et al. (2021). Reviews and syntheses: Arctic fire regimes and emissions in the 21st century. *Biogeosciences*, *18*(18), 5053–5083. https://doi.org/10.5194/bg-18-5053-2021

McCoy, D. T., Bender, F. A. M., Grosvenor, D. P., Mohrmann, J. K., Hartmann, D. L., Wood, R., & Field, P. R. (2018). Predicting decadal trends in cloud droplet number concentration using reanalysis and satellite data. *Atmospheric Chemistry and Physics*, *18*(3), 2035–2047. https://doi.org/10.5194/acp-18-2035-2018

Mielonen, T., Aaltonen, V., Lihavainen, H., Hyvärinen, A. P., Arola, A., Komppula, M., & Kivi, R. (2013). Biomass burning aerosols observed in Northern Finland during the 2010 wildfires in Russia. *Atmosphere*, *4*(1), 17–34. https://doi.org/10.3390/atmos4010017

Mielonen, T., Portin, H., Komppula, M., Leskinen, A., Tamminen, J., Ialongo, I., et al. (2012). Biomass burning aerosols observed in Eastern Finland during the Russian wildfires in summer 2010—Part 2: Remote sensing. *Atmospheric Environment*, *47*, 279–287. https://doi.org/10.1016/j.atmosenv.2011.07.016

MODIS/Aqua Terra Thermal Anomalies/Fire locations 1km FIRMS V006 NRT (Vector data). (2015). The land, atmosphere near real-time capability for EOS (LANCE). https://doi.org/10.5067/FIRMS/MODIS/MCD14DL.NRT.006

Moroni, B., Cappelletti, D., Crocchianti, S., Becagli, S., Caiazzo, L., Traversi, R., et al. (2017). Morphochemical characteristics and mixing state of long range transported wildfire particles at Ny-Ålesund (Svalbard Islands). *Atmospheric Environment*, *156*(March), 135–145. https://doi.org/10.1016/j.atmosenv.2017.02.037

Niemi, J. V., Tervahattu, H., Vehkamäki, H., Kulmala, M., Koskentalo, T., Sillanpää, M., & Rantamäki, M. (2004). Characterization and source identification of a fine particle episode in Finland. *Atmospheric Environment*, *38*(30), 5003–5012. https://doi.org/10.1016/j.atmosenv.2004.06.023

Petters, M. D., & Kreidenweis, S. M. (2007). A single parameter representation of hygroscopic growth and cloud condensation nucleus activity. *Atmospheric Chemistry and Physics*, *13*(2), 1081–1091. https://doi.org/10.5194/acp-7-1961-2007

Platnick, S., Ackerman, S., & King, M. (2017). *MODIS atmosphere L2 cloud product (06_L2)*. NASA MODIS Adaptive Processing System, Goddard Space Flight Center. https://doi.org/10.5067/MODIS/MOD06_L2.061

Platnick, S., King, M. D., Ackerman, S. A., Menzel, W. P., Baum, B. A., Riédi, J. C., & Frey, R. A. (2003). The MODIS cloud products: Algorithms and examples from TERRA. *IEEE Transactions on Geoscience and Remote Sensing*, *41*, 459–472. https://doi.org/10.1109/TGRS.2002.808301

Platt, S. M., Hov, Ø., Berg, T., Breivik, K., Eckhardt, S., Eleftheriadis, K., et al. (2022). Atmospheric composition in the European Arctic and 30 years of the Zeppelin observatory, Ny-Ålesund. *Atmospheric Chemistry and Physics*, *22*(5), 3321–3369. https://doi.org/10.5194/acp-22-3321-2022

Pöhlker, M. L., Ditas, F., Saturno, J., Klimach, T., Hrabě De Angelis, I., Araùjo, A. C., et al. (2018). Long-term observations of cloud condensation nuclei over the Amazon rain forest—Part 2: Variability and characteristics of biomass burning, long-range transport, and pristine rain forest aerosols. *Atmospheric Chemistry and Physics*, *18*(14), 10289–10331. https://doi.org/10.5194/acp-18-10289-2018

Portin, H., Leskinen, A., Hao, L., Kortelainen, A., Miettinen, P., Jaatinen, A., et al. (2014). The effect of local sources on particle size and chemical composition and their role in aerosol-cloud interactions at Puijo measurement station. *Atmospheric Chemistry and Physics*, *14*(12), 6021–6034. https://doi.org/10.5194/acp-14-6021-2014

Portin, H., Mielonen, T., Leskinen, A., Arola, A., Pärjälä, E., Romakkaniemi, S., et al. (2012). Biomass burning aerosols observed in Eastern Finland during the Russian wildfires in summer 2010—Part 1: In-situ aerosol characterization. *Atmospheric Environment*, *47*, 269–278. https://doi.org/10.1016/j.atmosenv.2011.10.067

Ramanathan, V., Crutzen, P. J., Kiehl, J. T., & Rosenfeld, D. (2001). Aerosols climate and the hydrological cylce. *Science*, *294*, 2119–2125. https://doi.org/10.1126/science.1064034

Reid, J. S., Koppmann, R., Eck, T. F., & Eleuterio, D. P. (2005). A review of biomass burning emissions part II: Intensive physical properties of biomass burning particles. *Atmospheric Chemistry and Physics*, *5*(3), 799–825. https://doi.org/10.5194/acp-5-799-2005

Rejano, F., Casquero-Vera, J. A., Lyamani, H., Andrews, E., Casans, A., Pérez-Ramírez, D., et al. (2023). Impact of urban aerosols on the cloud condensation activity using a clustering model. *Science of the Total Environment*, *858*, 159657. https://doi.org/10.1016/j.scitotenv.2022.159657

Rickards, A. M. J., Miles, R. E. H., Davies, J. F., Marshall, F. H., & Reid, J. P. (2013). Measurements of the sensitivity of aerosol hygroscopicity and the κ parameter to the O/C ratio. *Journal of Physical Chemistry A*, *117*(51), 14120–14131. https://doi.org/10.1021/jp407991n

Ross, K. E., Piketh, S. J., Bruintjes, R. T., Burger, R. P., Swap, R. J., & Annegarn, H. J. (2003). Spatial and aerosol variations in CCN distribution and the aerosol-CCN relationship over southern Africa. *Journal of Geophysical Research: Atmospheres*, *108*(13). https://doi.org/10.1029/2002jd002384

Saarnio, K., Aurela, M., Timonen, H., Saarikoski, S., Teinilä, K., Mäkelä, T., et al. (2010). Chemical composition of fine particles in fresh smoke plumes from boreal wild-land fires in Europe. *Science of the Total Environment*, *408*(12), 2527–2542. https://doi.org/10.1016/j.scitotenv.2010.03.010

Sakamoto, K. M., Allan, J. D., Coe, H., Taylor, J. W., Duck, T. J., & Pierce, J. R. (2015). Aged boreal biomass-burning aerosol size distributions from BORTAS 2011. *Atmospheric Chemistry and Physics*, *15*(4), 1633–1646. https://doi.org/10.5194/acp-15-1633-2015

Schmale, J., Henning, S., Decesari, S., Henzing, B., Keskinen, H., Sellegri, K., et al. (2018). Long-term cloud condensation nuclei number concentration, particle number size distribution and chemical composition measurements at regionally representative observatories. *Atmospheric Chemistry and Physics*, *18*(4), 2853–2881. https://doi.org/10.5194/acp-18-2853-2018

Shrestha, B., Brotzge, J. A., & Wang, J. (2022). Observations and impacts of long-range transported wildfire smoke on air quality across New York state during July 2021. *Geophysical Research Letters*, *49*(19), 1–11. https://doi.org/10.1029/2022GL100216

Sillanpää, M., Saarikoski, S., Hillamo, R., Pennanen, A., Makkonen, U., Spolnik, Z., et al. (2005). Chemical composition, mass size distribution and source analysis of long-range transported wildfire smokes in Helsinki. *Science of the Total Environment*, *350*(1–3), 119–135. https://doi.org/10.1016/j.scitotenv.2005.01.024

Sporre, M. K., Swietlicki, E., Glantz, P., & Kulmala, M. (2014). Aerosol indirect effects on continental low-level clouds over Sweden and Finland. *Atmospheric Chemistry and Physics*, *14*(22), 12167–12179. https://doi.org/10.5194/acp-14-12167-2014

Spracklen, D. V., Carslaw, K. S., Pöschl, U., Rap, A., & Forster, P. M. (2011). Global cloud condensation nuclei influenced by carbonaceous combustion aerosol. *Atmospheric Chemistry and Physics*, *11*(17), 9067–9087. https://doi.org/10.5194/acp-11-9067-2011

Stein, A. F., Draxler, R. R., Rolph, G. D., Stunder, B. J. B., Cohen, M. D., & Ngan, F. (2015). NOAA'S hysplit atmospheric transport and dispersion modeling system. *Bulletin of the American Meteorological Society*, *96*(12), 2059–2077. https://doi.org/10.1175/BAMS-D-14-00110.1

Stohl, A., Berg, T., Burkhart, J. F., Fjæraa, A. M., Forster, C., Herber, A., et al. (2007). Arctic smoke—Record high air pollution levels in the European Arctic due to agricultural fires in Eastern Europe in spring 2006. *Atmospheric Chemistry and Physics*, *7*(2), 511–534. https://doi.org/10.5194/acp-7-511-2007

Suda, S. R., Petters, M. D., Matsunaga, A., Sullivan, R. C., Ziemann, P. J., & Kreidenweis, S. M. (2012). Hygroscopicity frequency distributions of secondary organic aerosols. *Journal of Geophysical Research*, *117*(4), 1–14. https://doi.org/10.1029/2011JD016823

Takeishi, A., Storelvmo, T., & Fierce, L. (2020). Disentangling the microphysical effects of fire particles on convective clouds through A case study. *Journal of Geophysical Research: Atmospheres*, *125*(12). https://doi.org/10.1029/2019JD031890

Twohy, C. H., Toohey, D. W., Levin, E. J. T., DeMott, P. J., Rainwater, B., Garofalo, L. A., et al. (2021). Biomass burning smoke and its influence on clouds over the Western U. S. *Geophysical Research Letters*, *48*(15), 1–10. https://doi.org/10.1029/2021GL094224

Tyukavina, A., Potapov, P., Hansen, M. C., Pickens, A. H., Stehman, S. V., Turubanova, S., et al. (2022). Global trends of forest loss due to fire from 2001 to 2019. *Frontiers in Remote Sensing*, *3*(March), 1–20. https://doi.org/10.3389/frsen.2022.825190

Väisänen, O., Ruuskanen, A., Ylisirniö, A., Miettinen, P., Portin, H., Hao, L., et al. (2016). In-cloud measurements highlight the role of aerosol hygroscopicity in cloud droplet formation. *Atmospheric Chemistry and Physics*, *16*(16), 10385–10398. https://doi.org/10.5194/acp-16-10385-2016

Vakkari, V. (2014). Rapid changes in biomass burning aerosols by atmospheric oxidation. *Geophysical Prospecting*, 6413–6419. https://doi.org/10.1002/2014GL061184.Received

Wu, Z. J., Zheng, J., Shang, D. J., Du, Z. F., Wu, Y. S., Zeng, L. M., et al. (2016). Particle hygroscopicity and its link to chemical composition in the urban atmosphere of Beijing, China, during summertime. *Atmospheric Chemistry and Physics*, *16*(2), 1123–1138. https://doi.org/10.5194/acp-16-1123-2016

Xu, W., He, Y., Qiu, Y., Chen, C., Xie, C., Lei, L., et al. (2020). Mass spectral characterization of primary emissions and implications in source apportionment of organic aerosol. *Atmospheric Measurement Techniques*, *13*(6), 3205–3219. https://doi.org/10.5194/amt-13-3205-2020

Zheng, G., Sedlacek, A. J., Aiken, A. C., Feng, Y., Watson, T. B., Raveh-Rubin, S., et al. (2020). Long-range transported North American wildfire aerosols observed in marine boundary layer of eastern North Atlantic. *Environment International*, *139*, 105680. https://doi.org/10.1016/j.envint.2020.105680

References From the Supporting Information

Allison, C. A., DeCarlo, P. F., & Jimenez, J. L. (2007). Elemental analysis of organic species with electron ionization high-resolution mass spectrometry. *Analytical Chemistry*, *3*(1), 301–310. https://doi.org/10.1021/ac071150w

Canagaratna, M. R., Jimenez, J. L., Kroll, J. H., Chen, Q., Kessler, S. H., Massoli, P., et al. (2015). Elemental ratio measurements of organic compounds using aerosol mass spectrometry: Characterization, improved calibration, and implications. *Atmospheric Chemistry and Physics*, *15*(1), 253–272. https://doi.org/10.5194/acp-15-253-2015

DeCarlo, P. F., Kimmel, J. R., Trimborn, A., Northway, M. J., Jayne, J. T., Aiken, A. C., et al. (2006). Field-deployable, high-resolution, time-of-flight aerosol mass spectrometer. *Analytical Chemistry*, *78*(24), 8281–8289. https://doi.org/10.1021/ac061249n

Fan, X., Liu, J., Zhang, F., Chen, L., Collins, D., Xu, W., et al. (2020). Contrasting size-resolved hygroscopicity of fine particles derived by HTDMA and HR-ToF-AMS measurements between summer and winter in Beijing: The impacts of aerosol aging and local emissions. *Atmospheric Chemistry and Physics*, *20*(2), 915–929. https://doi.org/10.5194/acp-20-915-2020

Gramlich, Y., Siegel, K., Haslett, S. L., Freitas, G., Krejci, R., Zieger, P., & Mohr, C. (2023). Revealing the chemical characteristics of Arctic low-level cloud residuals—In situ observations from a mountain site. *Atmospheric Chemistry and Physics*, *23*, 1–29. https://doi.org/10.5194/acp-23-6813-2023

Gryspeerdt, E., Quaas, J., & Bellouin, N. (2016). Constraining the aerosol influence on cloud fraction. *Journal of Geophysical Research: Atmospheres*, *121*(7), 3566–3583. https://doi.org/10.1002/2015JD023744

Gysel, M., Crosier, J., Topping, D. O., Whitehead, J. D., Bower, K. N., Cubison, M. J., et al. (2007). Closure study between chemical composition and hygroscopic growth of aerosol particles during TORCH2. *Atmospheric Chemistry and Physics*, *7*(24), 6131–6144. https://doi.org/10.5194/acp-7-6131-2007

Jaatinen, A., Romakkaniemi, S., Hao, L. Q., Kortelainen, A., Miettinen, P., Mikkonen, S., et al. (2014). The third Pallas Cloud Experiment: Consistency between the aerosol hygroscopic growth and CCN activity. *Boreal Environment Research*, *19*, 368–382.

Koike, M., Ukita, J., Ström, J., Tunved, P., Shiobara, M., Vitale, V., et al. (2019). Year-round in situ measurements of Arctic low-level clouds: Microphysical properties and their relationships with aerosols. *Journal of Geophysical Research: Atmospheres*, *124*(3), 1798–1822. https://doi.org/10.1029/2018JD029802

Lee, B. H., Lopez-Hilfiker, F. D., Mohr, C., Kurtén, T., Worsnop, D. R., & Thornton, J. A. (2014). An iodide-adduct high-resolution time-of-flight chemical-ionization mass spectrometer: Application to atmospheric inorganic and organic compounds. *Environmental Science and Technology*, *48*(11), 6309–6317. https://doi.org/10.1021/es500362a

Lopez-Hilfiker, F. D., Mohr, C., Ehn, M., Rubach, F., Kleist, E., Wildt, J., et al. (2014). A novel method for online analysis of gas and particle composition: Description and evaluation of a filter inlet for gases and AEROsols (FIGAERO). *Atmospheric Measurement Techniques*, *7*(4), 983–1001. https://doi.org/10.5194/amt-7-983-2014

Müller, T., Henzing, J. S., De Leeuw, G., Wiedensohler, A., Alastuey, A., Angelov, H., et al. (2011). Characterization and intercomparison of aerosol absorption photometers: Result of two intercomparison workshops. *Atmospheric Measurement Techniques*, *4*(2), 245–268. https://doi.org/10.5194/amt-4-245-2011

Ng, N. L., Herndon, S. C., Trimborn, A., Canagaratna, M. R., Croteau, P. L., Onasch, T. B., et al. (2011). An Aerosol Chemical Speciation Monitor (ACSM) for routine monitoring of the composition and mass concentrations of ambient aerosol. *Aerosol Science and Technology*, *45*(7), 780–794. https://doi.org/10.1080/02786826.2011.560211

Ohata, S., Mori, T., Kondo, Y., Sharma, S., Hyvärinen, A., Andrews, E., et al. (2021). Estimates of mass absorption cross sections of black carbon for filter-based absorption photometers in the Arctic. *Atmospheric Measurement Techniques*, *14*(10), 6723–6748. https://doi.org/10.5194/amt-14-6723-2021

Paatero, P., & Tapper, U. (1994). Positive matrix factorization: A non-negative factor model with optimal utilization of error estimates of data values. *Environmetrics*, *5*(2), 111–126. https://doi.org/10.1002/env.3170050203

Pasquier, J. T., David, R. O., Freitas, G., Gierens, R., Gramlich, Y., Haslett, S., et al. (2022). The Ny-Ålesund aerosol cloud experiment (NASCENT): Overview and first results. *Bulletin of the American Meteorological Society*, *103*(11), E2533–E2558. https://doi.org/10.1175/bams-d-21-0034.1

Siegel, K., Gramlich, Y., Haslett, S. L., Freitas, G., Krejci, R., & Mohr, C. (2023). Arctic observations of Hydroperoxymethyl Thioformate (HPMTF)—Seasonal behavior and relationship to other oxidation products from Dimethyl Sulfide at the Zeppelin Observatory, Svalbard, (February).

Tørseth, K., Aas, W., Breivik, K., Fjeraa, A. M., Fiebig, M., Hjellbrekke, A. G., et al. (2012). Introduction to the European Monitoring and Evaluation Programme (EMEP) and observed atmospheric composition change during 1972–2009. *Atmospheric Chemistry and Physics*, *12*(12), 5447–5481. https://doi.org/10.5194/acp-12-5447-2012

Tunved, P., Ström, J., & Krejci, R. (2013). Arctic aerosol life cycle: Linking aerosol size distributions observed between 2000 and 2010 with air mass transport and precipitation at Zeppelin station, Ny-Ålesund, Svalbard. *Atmospheric Chemistry and Physics*, *13*(7), 3643–3660. https://doi.org/10.5194/acp-13-3643-2013

Ulbrich, I. M., Canagaratna, M. R., Zhang, Q., Worsnop, D. R., & Jimenez, J. L. (2009). Interpretation of organic components from Positive Matrix Factorization of aerosol mass spectrometric data. *Atmospheric Chemistry and Physics*, *9*(9), 2891–2918. https://doi.org/10.5194/acp-9-2891-2009